

GRANULITE-FACIES CONDITIONS PRESERVED IN VANADIUM- AND CHROMIUM-RICH METAPELITES FROM THE PARADISE BASIN, WIND RIVER RANGE, WYOMING, U.S.A.

CASEY L. DONOHUE[§] AND ERIC J. ESSENE[¶]

Department of Geological Sciences, University of Michigan, Ann Arbor, Michigan 48109-1063, U.S.A.

ABSTRACT

Metapelites with unusually high levels of several transition elements, including V, Cr and Zn, have been found in Archean rocks from the Paradise Basin area of the Wind River Range, Wyoming. These rocks contain sillimanite with up to 0.56 wt% V₂O₃ and 0.32% Cr₂O₃. Coexisting minerals are also enriched in V and Cr, including garnet, hercynite and biotite. The K_D values for V and Cr *versus* Al have been calculated among garnet, sillimanite and hercynite. The partitioning of V/Al is nearly equal ($K_D = 0.98$) between garnet and sillimanite, whereas Cr/Al is strongly favored by garnet ($K_D = 6.9$). Hercynite strongly partitions V/Al over both garnet and sillimanite ($K_D \approx 15$) and very strongly partitions Cr/Al over garnet and sillimanite (K_D of 27 and 189, respectively). The hercynite also contains most of the Zn in the rock, as 10% of the gahnite component in solid solution. The P–T conditions recorded in the cores of matrix minerals indicate peak metamorphism in the granulite facies at $>9.5 \pm 0.1$ kbar and $780 \pm 50^\circ\text{C}$. Rim compositions in the matrix indicate lower-grade conditions that constrain a portion of the retrograde P–T path. There is no evidence of introduction of elements along veins or fractures, and the source of the V, Cr, and Zn is presumably provided by weathering of older source materials that were deposited as clastic grains.

Keywords: granulites, vanadium, metapelite, Wind River Range, Wyoming.

SOMMAIRE

Nous documentons la présence de métapelites ayant des niveaux anormalement élevés de plusieurs éléments de transition, y inclus V, Cr and Zn, dans une suite de roches archéennes de la région de Paradise Basin, dans la chaîne de Wind River, au Wyoming. Ce sont des roches à sillimanite contenant jusqu'à 0.56% de V₂O₃ et 0.32% de Cr₂O₃. Les minéraux coexistants sont aussi enrichis en V et Cr, y inclus le grenat, la hercynite et la biotite. Nous avons calculé les valeurs de K_D pour V et Cr par rapport à Al pour le grenat, la sillimanite et la hercynite. La répartition de V/Al entre grenat et sillimanite est à peu près égale ($K_D = 0.98$), tandis que Cr/Al est fortement favorisé par le grenat ($K_D = 6.9$). La hercynite favorise fortement V/Al par rapport à grenat et sillimanite (K_D égal à 15) et Cr/Al par rapport à grenat et sillimanite (K_D égal à 27 et 189, respectivement). La hercynite contient en plus la plupart du zinc, sous forme de la composante gahnite, formant jusqu'à 10% d'une solution solide. Les conditions P–T enregistrées dans le coeur des minéraux de la matrice indiquent un paroxysme métamorphique au faciès granulite, à plus de 9.5 ± 0.1 kbar et $780 \pm 50^\circ\text{C}$. Dans cette matrice, la composition de la bordure des minéraux indique des conditions de plus faible intensité qui définissent une portion du tracé P–T lors de la rétrogression. Il n'y a aucune évidence d'introduction d'éléments le long de veines ou de fractures; les quantités inhabituelles de V, Cr, et Zn seraient fournies par lessivage de matériaux plus anciens, déposés sous forme de grains clastiques.

(Traduit par la Rédaction)

Mots-clés: granulites, vanadium, métapélite, chaîne de Wind River, Wyoming.

[§] *Present address:* Exxon Mobil Exploration Co., Houston, Texas 77060, U.S.A.

E-mail address: casey.l.donohue@exxonmobil.com

[¶] *E-mail address:* essene@umich.edu

INTRODUCTION

Although the aluminosilicate polymorphs commonly occur as nearly pure Al_2SiO_5 , many authors have noted trace- and minor-element substitutions in all three polymorphs. Substitutions into the aluminosilicates may be significant because of the large number of thermo-barometric reactions that contain these phases. Despite their prevalence, these minerals are rarely analyzed by investigators, and their composition is usually assumed to be ideal. The most common substitution in all three aluminosilicates is $\text{Fe}^{3+}\text{Al}_{-1}$, although other transition elements (Mn^{3+} , V^{3+} , Ti , Cr^{3+}) may also be found at minor and trace levels (Strens 1968). Although some investigators have reported minor to trace levels of Na, P and K in aluminosilicates (*e.g.*, Dodge 1971), these elements are likely attributable to tiny inclusions of other phases rather than substitutions in the aluminosilicates.

Andalusite is known to incorporate wt% levels of Mn_2O_3 and Fe_2O_3 (*e.g.*, Okrusch & Evans 1970, Dodge 1971), as well as 1–2 wt% V_2O_3 and Cr_2O_3 (Morand 1988). Vrana *et al.* (1978) described kanonaite as a new species (ideally $\text{Mn}^{3+}\text{AlSiO}_5$), with up to 32.2 wt% Mn_2O_3 , that is isotypic with andalusite. Kyanite has been shown to contain several wt% Cr_2O_3 (*e.g.*, Cooper 1980, Gil Ibarguchi *et al.* 1991) and Fe_2O_3 (*e.g.*, Deer *et al.* 1982). Sobolev *et al.* (1968) reported very high levels of Cr (12.9 wt% Cr_2O_3) in kyanite from grosspyrite xenoliths in a kimberlite from Yakutia. Sillimanite with up to several wt% Fe_2O_3 is well known and has been reported by numerous authors. For instance, Grew (1980) investigated reactions between ilmenite and sillimanite in granulite- and amphibolite-facies rocks, where the aluminosilicate contains up to 1.8 wt% Fe_2O_3 . He showed that it is buffered in sillimanite by the reaction $\text{SiO}_2 + \text{Fe}_2\text{O}_3 + \text{Al}_2\text{SiO}_5 = 2\text{FeAlSiO}_5$. Other transition metals have been reported at minor and trace levels by a few investigators. Okrusch & Evans (1970) established the minor element content of sillimanite coexisting with andalusite, and reported up to 0.2 wt% V_2O_3 and 0.2 wt% Cr_2O_3 . Dodge (1971) also reported up to 0.67 wt% Fe_2O_3 and approximately 1100 ppm (0.1 wt%) of both Cr_2O_3 and V_2O_3 in sillimanite determined by wet-chemical analysis.

In this paper, we describe an occurrence of V- and Cr-rich oxides and silicates, most notably vanadoan sillimanite, in upper-amphibolite- to granulite-facies metapelites from the Paradise Basin area of the Wind River Range (WRR) of Wyoming (Figs. 1a, b). These unusual rocks are part of a rare sequence of Archean supracrustal units found in several locations within the WRR, which locally include metapelite, metabasalt, pelitic gneiss, and iron formation (Frost *et al.* 2000, Sharp & Essene 1991). The large Archean core of the range, which consists mostly of orthogneisses, migmatites, and granites, has become exposed at the surface owing to late Cretaceous to early Tertiary

Laramide thrusting. Frost *et al.* (1998) delineated a long-lived plutonic history of the range that extended for at least 250 Ma in the Archean, from ~2.8 to 2.55 Ga.

FIELD RELATIONSHIPS

The Precambrian rocks of the Paradise Basin area, largely gneisses and granites, have been divided into eight metamorphic stratigraphic units. A simplified bedrock-geology map of the area, based largely on the mapping of Perry (1965), is shown in Figure 1b. The majority of the highly aluminous gneisses (the focus of this report) are found within the St. Lawrence Creek gneiss, including samples 01-PB-2, 01-PB-16, 01-PB-17a and 01-PB-20. This unit is suspected to have a sedimentary origin owing to aluminum enrichment and persistent layering of the larger units over distances of 8–9 km (Perry 1965). Amphibolite boudins are found throughout the Basin, cutting all units, but are most plentiful within the Eric Lake gneiss. These units likely have a mafic volcanic origin. Samples 01-PB-6a and 01-PB-8a are from a large mafic boudin within the Sheep Mountain gneiss.

MINERAL ASSEMBLAGES AND COMPOSITIONS

The mineral assemblages for several metapelites collected from the Paradise Basin are shown in Table 1.

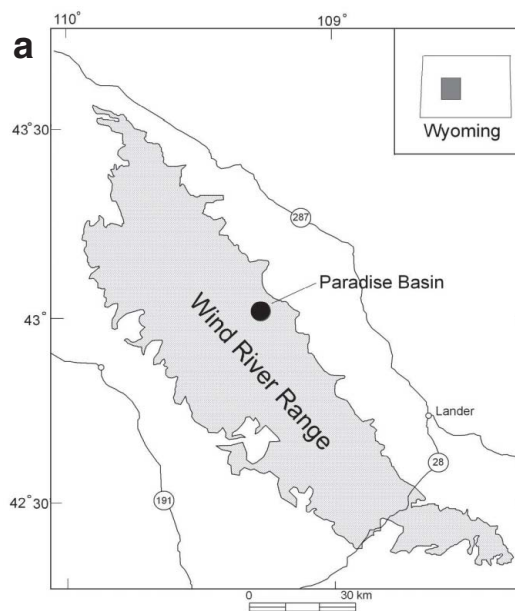
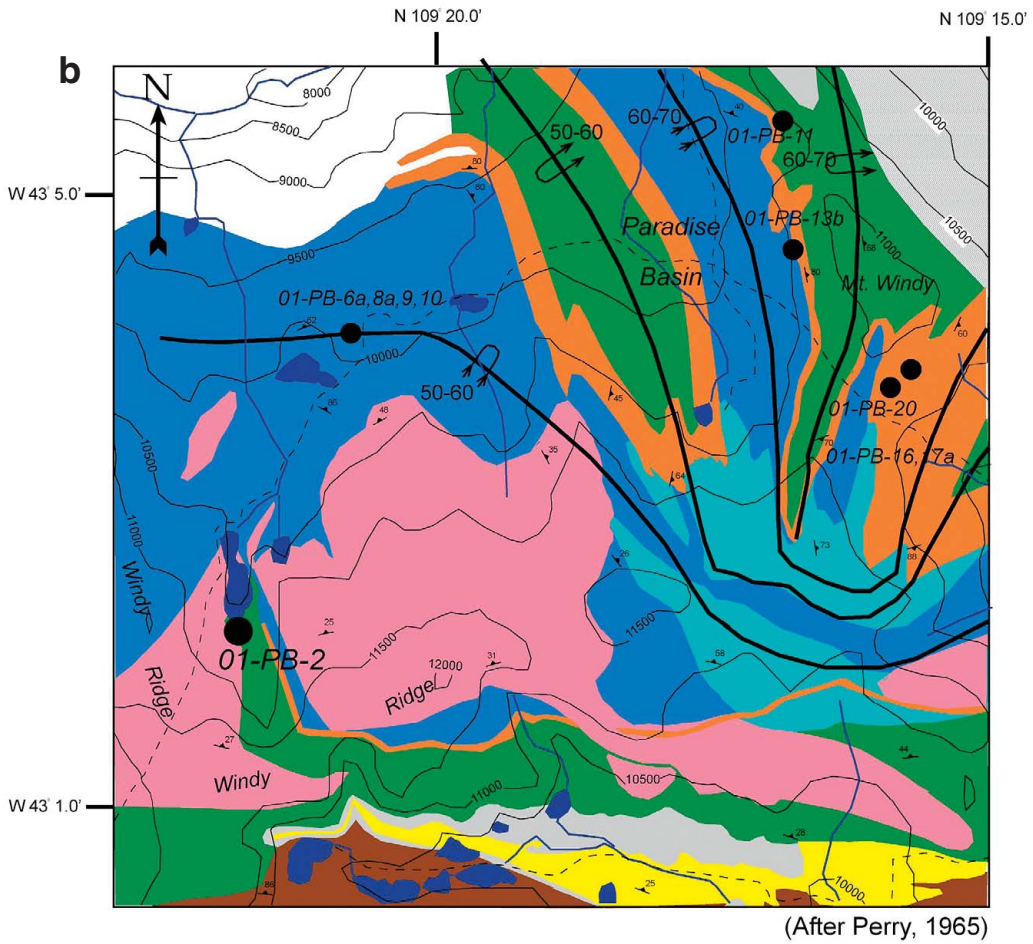
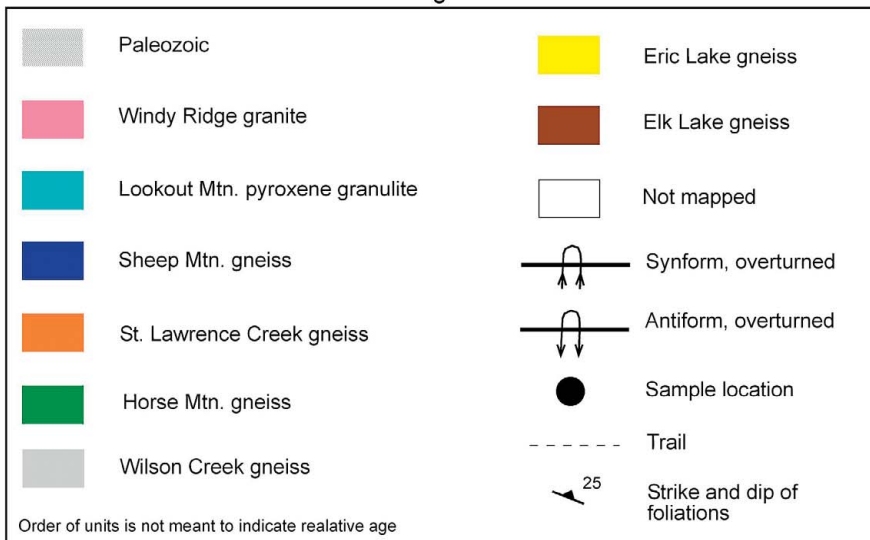


FIG. 1. a) Map showing the location of the Paradise Basin within the Wind River Range in Wyoming. b) Map showing the bedrock geology of the Paradise Basin area.



Legend



The focus of this paper, however, is directed toward the low-variance metapelitic assemblage with anomalous vanadium and chromium in sample 01-PB-2. The mineral assemblage of the metapelitic sample 01-PB-2 consists of biotite, cordierite, garnet, hercynite, ilmenite, K-feldspar, muscovite, plagioclase, quartz and sillimanite. There are many accessory phases, including apatite, allanite, graphite, monazite, pyrrhotite and zircon. Minerals (biotite, garnet, hercynite, ilmenite, and sillimanite) with unusually high V and Cr contents are described and analyzed in this paper; details of the analytical technique are presented in Appendix A.

Sillimanite

Sillimanite occurs in sample 01-PB-2 as numerous small, colorless and generally elongate inclusions (approximately $2 \times 10 \mu\text{m}$ in size) in garnet porphyroblasts as well as rare larger subhedral matrix grains (Figs. 2a, b). Sillimanite inclusions in garnet were characterized with X-ray analysis as well as Raman spectroscopy. The X-ray determination was conducted using a single grain of garnet containing numerous aluminosilicate inclusions; it was extracted from a thin section and mounted on a glass fiber. This assembly was run in a Gandolfi camera for 24 hours. An Fe X-ray source was utilized at 40 kV and 15 nA in order to eliminate fluorescence by Fe from the garnet matrix. Interferences from garnet were few and were easily identified in the pattern. Although only a few lines were found, the three strongest

reflections for sillimanite ($d = 3.420, 3.366, 2.210 \text{ \AA}$, respectively) that were identified are in good agreement in terms of both position and intensity with the pattern described in the *Mineral Powder Diffraction File* for sillimanite (Table 2). The identification of sillimanite was confirmed by the use of *in situ* Raman spectroscopy. Inclusions of sillimanite in garnet were run on a micro-Raman apparatus equipped with an Ar-ion 514 nm coherent laser. Count times ranged from 45 to 1800 seconds with power settings between 1000 and 1750 mW. All samples were run with a $10\times$ objective lens, mid-confocal setting, a horizontal slit-width of $140 \mu\text{m}$, and a 600 holographic spectrometer grating. Analyses of sillimanite inclusions show peaks at wavenumbers 232.2, 308, and 968.9 cm^{-1} , which is consistent with the three strongest peaks measured for a sillimanite standard.

The elements V, Cr, and Fe are easily detected in the sillimanite with EDS scans run for 60 seconds at 30 nA and 15 kV when the intensity scale is amplified. Results of electron-microprobe analyses of the garnet-hosted sillimanite inclusions from sample 01-PB-2 are shown in Table 3. The sillimanite inclusions contain up to 0.56 wt% V_2O_3 , 0.32 wt% Cr_2O_3 , and 1.13 wt% Fe_2O_3 . The levels of V and Cr in sillimanite reported here are the highest known to the authors. Compositions of matrix sillimanite are lower in minor elements, with $<0.2 \text{ wt}\%$ Fe_2O_3 , $<0.3 \text{ wt}\%$ V_2O_3 and $<0.2 \%$ Cr_2O_3 (Table 2).

Garnet

The garnet in sample 01-PB-2 is virtually unzoned with respect to major elements and has an average composition $\text{Alm}_{78}\text{Prp}_{17}\text{Sps}_2\text{Grs}_3$ (Table 4). Multiple analytical traverses were conducted to assess potential zoning, although nearly flat compositional profiles were observed except at the immediate rim ($0\text{--}10 \mu\text{m}$), where obvious retrograde exchange occurred. Texturally, there appear to be two separate populations of porphyroblastic garnet. The smaller grains of garnet commonly contain inclusions of sillimanite, quartz, K-feldspar, hercynite, ilmenite, monazite and plagioclase, and are darker red in color. Many of the larger grains, which are up to 5 mm in diameter, contain numerous inclusions of quartz, K-feldspar, biotite, and plagioclase, but never sillimanite, and are an orange-red color. Five separate thin sections from the same sample were cut and examined optically and *via* back-scattered electron images in order to accurately assess the assemblages of inclusions as well as to insure that the smaller grains of garnet were not merely the edges of larger grains. It is unclear whether the population of larger grains (containing no sillimanite inclusions) is in equilibrium with sillimanite, as no inclusions of sillimanite are found within them, and no matrix sillimanite was found in direct contact with the larger grains of garnet.

Keane (1997) noted disparate trace-element profiles (using SIMS analysis) in two grains of garnet with com-

TABLE 1. MINERAL ASSEMBLAGES OF ROCKS FROM THE PARADISE BASIN, WIND RIVER RANGE, WYOMING

Sample	Type	Mineral assemblage
01-PB-2	pelitic	aln, ap, bt, crd, gr, grt, hc, ilm, kfs, mnz, (ms), pl, po, rt, qtz, sil, zrn
01-PB-6a	mafic	hbl, ilm, (ms), pl, qtz
01-PB-8a	mafic	(chl), hbl, ilm, (ms), pl, qtz
01-PB-9	felsic	bt, crd, (hem), ilm, kfs, ms, pl, qtz, zrn
01-PB-10	felsic	bt, (chl), ilm, kfs, (ms), pl, qtz
01-PB-11	felsic	bt, crd, ms, pl, qtz, zrn
01-PB-13b	pelitic	bt, grt, hc, ilm, kfs, mnz, (ms), pl, po, qtz, sil, zrn
01-PB-16	pelitic	bt, crd, grt, (ms), pl, qtz, (rt), zrn
01-PB-17a	pelitic	bt, crd, gr, grt, hc, ilm, kfs, mnz, (ms), pl, qtz, zrn
01-PB-20	pelitic	ap, bt, crd, grt, ilm, kfs, mnz, pl, qtz, (rt)

Symbols: aln: allanite, ap: apatite, bt: biotite, chl: chlorite, crd: cordierite, gr: graphite, grt: garnet, hem: hematite, hbl: hornblende, hc: hercynite, ilm: ilmenite, kfs: K-feldspar, mnz: monazite, ms: muscovite, pl: plagioclase, po: pyrrhotite, qtz: quartz, rt: rutile, sil: sillimanite, and zrn: zircon. Parentheses indicate a retrograde phase.

mon major-element profiles from a single thin section of a sample collected within 1 km of the location of sample 01-PB-2. He concluded that the two different trace-element profiles represent separate portions of a single prograde P-T path, although growth of garnet in two separate metamorphic events also is possible. Electron-microprobe analyses of the smaller porphyroblastic

grains of garnet in 01-PB-2 yield 0.05–0.10 (± 0.003) wt% V_2O_5 , 0.13–0.24 (± 0.02) wt% Cr_2O_3 , and 0.00–0.07 (± 0.004) wt% ZnO. The minor levels of V and Cr likely substitute into the octahedral site of garnet by goldmanite- ($Ca_3V_2Si_3O_{12}$) and uvarovite- ($Ca_3Cr_2Si_3O_{12}$) type substitutions, respectively. The larger grains of garnet have slightly higher pyrope and grossular

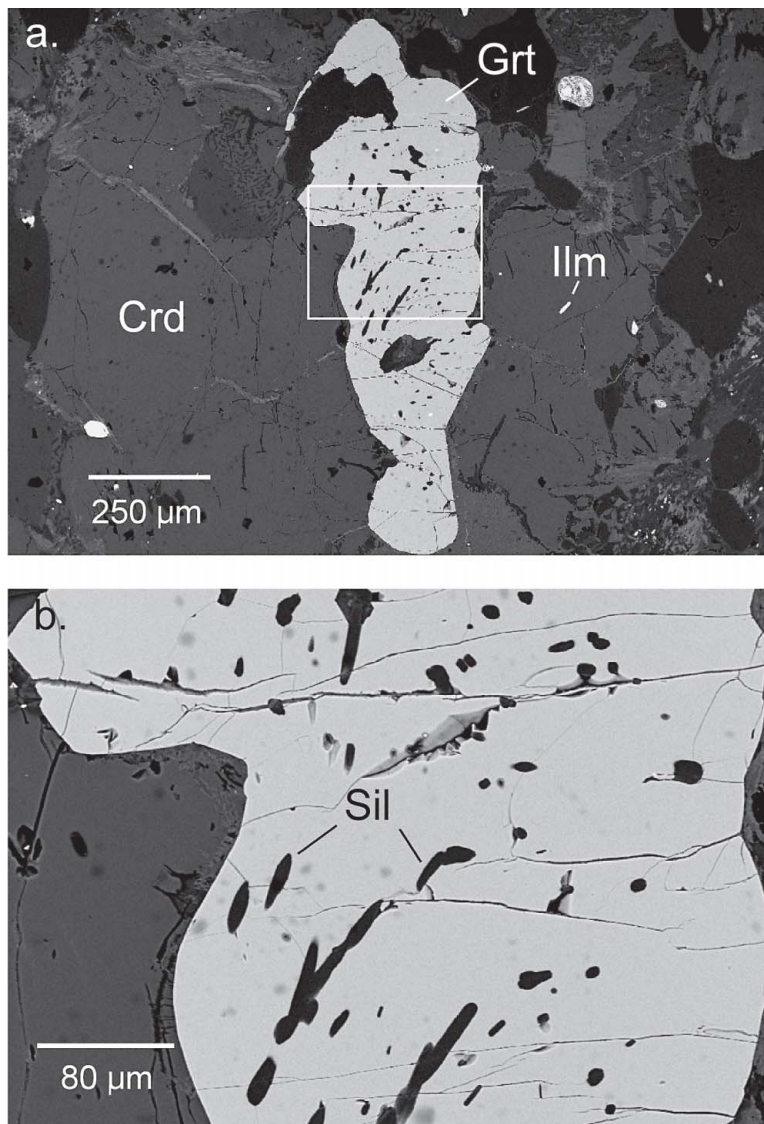


FIG. 2. BSE image of a garnet porphyroblast from sample 01-PB-2 with numerous inclusions of sillimanite. The white box in a) shows the boundaries of the enlarged area in b). Scale markers are shown at the bottom of both figures. Crd: cordierite, Grt: garnet, Ilm: ilmenite, Sil: sillimanite, Qtz: quartz.

contents, and comparable levels of trace and minor elements, compared to the smaller grains, although SIMS elemental profiles have not been measured for the garnet grains of 01-PB-2.

Biotite

Biotite occurs as both a matrix phase in sample 01-PB-2 as well as inclusions in garnet and quartz porphyroblasts. Most biotite grains appear to have retrogressively reacted with one or more of the other Fe-Mg-bearing minerals in the sample, such as garnet and cordierite. Figure 3 shows large laths of biotite growing at the expense of garnet. Matrix biotite grains also oc-

cur in a symplectitic intergrowth with quartz (Fig. 3), though the precursor phase for this assemblage is not known. The matrix biotite has a Mg# (Mg/Fe*100) of 68–80, with ~0.22 wt% V₂O₃, 2.24 wt% TiO₂ and ~0.24 wt% Cr₂O₃. The biotite grains included in garnet have lower Mg# (57–58), similar levels of TiO₂ (~2.1–2.2 wt%) and V₂O₃ and Cr₂O₃ contents of ~1.0 and 0.5 wt%, respectively. Biotite included in quartz appears to have been isolated from other mafic minerals and therefore has remained shielded from retrogressive exchange upon cooling. These inclusions preserve more Fe- and Ti-rich compositions, with a Mg# of ~46, and 0.41 wt% V₂O₃, 0.44 wt% Cr₂O₃ and 5.19 wt% TiO₂ (Table 5). Ferric iron in all biotite samples has been estimated as Fe³⁺ = Fe_{Total} * 0.04 based on the measurements of Guidotti & Dyar (1991) of biotite from graphite-buffered rocks.

TABLE 2. GANDOLFI XRD PATTERN FOR SILLIMANITE INCLUSIONS AND GARNET HOST

Line <i>hkl</i>	Relative intensity	<i>d</i> Å 01-PB	<i>d</i> Å PDF	Mineral
120	50	3.420	3.415	sil
210	20	3.366	3.366	sil
400	20	2.867	2.870	grt
420	100	2.563	2.569	grt
431	10	2.250	2.257	grt
122	15	2.210	2.204	sil
521	20	2.108	2.102	grt
440	15	2.026	2.020	grt

PDF: data from Mineral Powder Diffraction File. Databook, card #38-471. Symbols: sil: sillimanite, grt: garnet.

Feldspars

Plagioclase is found in both the matrix and as inclusions in garnet, whereas K-feldspar is found only in the matrix of the vanadium-rich schist. Representative compositions for the feldspars are shown in Table 6. The K-feldspar grains show perthitic exsolution lamellae (Fig. 4), which were re-integrated by conducting multiple rastered-beam microprobe analyses (15 μm × 15 μm raster) in order to recover the composition prior to exsolution. Thirty points were analyzed for each of eight K-feldspar grains, yielding the average composition

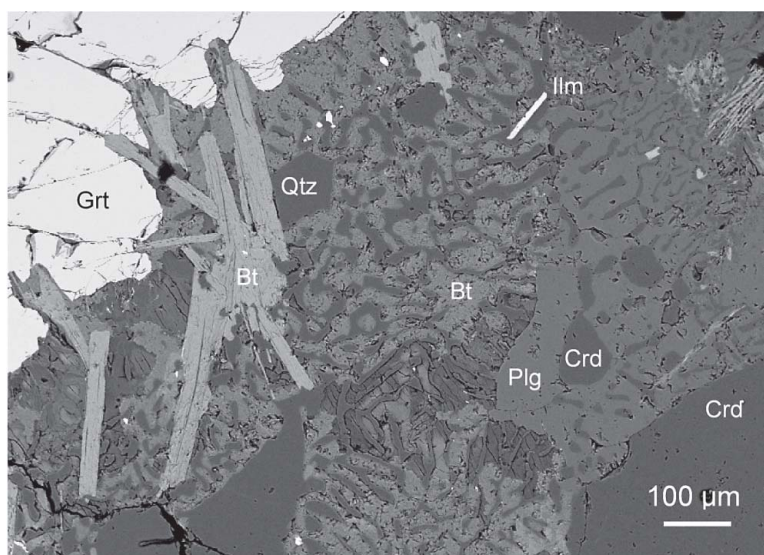


FIG. 3. BSE image of biotite-quartz and plagioclase-cordierite symplectites from 01-PB. Laths of biotite and anhedral garnet and cordierite also are present.

$\text{Kfs}_{88}\text{An}_{0.4}\text{Ab}_{12.5}$. Neither plagioclase nor K-feldspar contains measurable V or Cr.

Spinel

Sample 01–PB–2 contains chromian–zincian–vanadoan hercynite with up to 13.1 wt% Cr_2O_3 , 4.2 wt% ZnO and 2.7 wt% V_2O_3 (Table 6, Fig. 5). The end-member proportions for matrix and included spinels are shown in Table 7 and were calculated assuming that the spinel is all normal. The composition of the matrix spinel is approximately $\text{Hc}_{60}\text{Spl}_{10}\text{Chr}_{16}\text{Ghn}_{10}$, and the spinel grains included in garnet have the composition $\text{Hc}_{56}\text{Spl}_{15}\text{Chr}_{12}\text{Ghn}_{12}$.

Rutile

Rutile invariably occurs as inclusions in ilmenite, which suggests that it grew as the early Ti-oxide (Fig. 6). Rutile contains ~1.25 wt% V_2O_3 , 0.17 wt% Cr_2O_3 , and 0.85 wt% Fe_2O_3 (Table 8). In the absence of 5+ cations such as Nb, rutile accommodates substitution of R^{3+} as ROOH (*e.g.*, Wang *et al.* 1999). The Wind River rutile

has 0.013 VOOH, 0.000 CrOOH, 0.009 FeOOH, and 0.978 TiO_2 . Wang *et al.* (1999) obtained up to 0.011 VOOH, 0.065 CrOOH and 0.017 FeOOH in rutile found as inclusions in pyrope xenocrysts. Rudnick *et al.* (2000) reported up to 0.007 VOOH, 0.001 CrOOH and 0.020 FeOOH in rutile from granulites and eclogites. The lower FeOOH in the Wind River rutile may relate to its more reducing conditions.

Ilmenite

Ilmenite occurs as both overgrowths on rutile in the matrix as well as inclusions in the small porphyroblasts of garnet. The abundant ilmenite from this sample also contains unusually high levels of vanadium, with up to 0.75 wt% V_2O_3 (Table 7). The V is likely to substitute as V_2O_3 (karelianite solid-solution) in ilmenite under the relatively reducing conditions, indicated by the presence of graphite. The cation and anion charges are well balanced for ilmenite if all V is assumed to be trivalent. Schuiling & Feenstra (1980) showed that V typically occurs as 3+ in ilmenite below the hematite–magnetite oxygen buffer. These conditions are reasonable for this

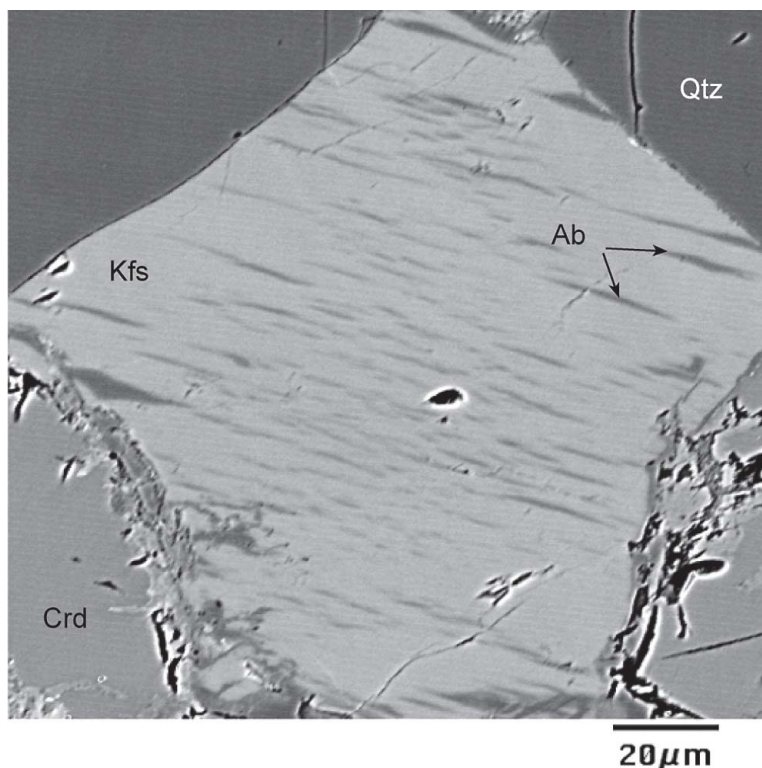


FIG. 4. BSE image of matrix K-feldspar (Ksp) grain with perthitic exsolution lamellae (Plg).

sample, although only an upper limit of QFM + 1 can be placed on the $\log f(\text{O}_2)$ in this sample by the stability of graphite (Ohmoto & Kerrick 1977).

Ilmenite has been shown to readily exchange Mg and Mn with other phases during cooling in high-grade rocks and is re-equilibrated at some P–T below peak conditions (Hayob *et al.* 1993). Therefore, we have estimated the composition of ilmenite at or near peak metamorphism for use in P–T calculations based on the core compositions of the large porphyroblasts of garnet. The K_D values for Mg/Fe between ilmenite and orthopyroxene from the experiments of Hayob *et al.* (1993) were combined with the K_D for garnet–orthopyroxene from Lee & Ganguly (1988) in a chain calculation as follows:

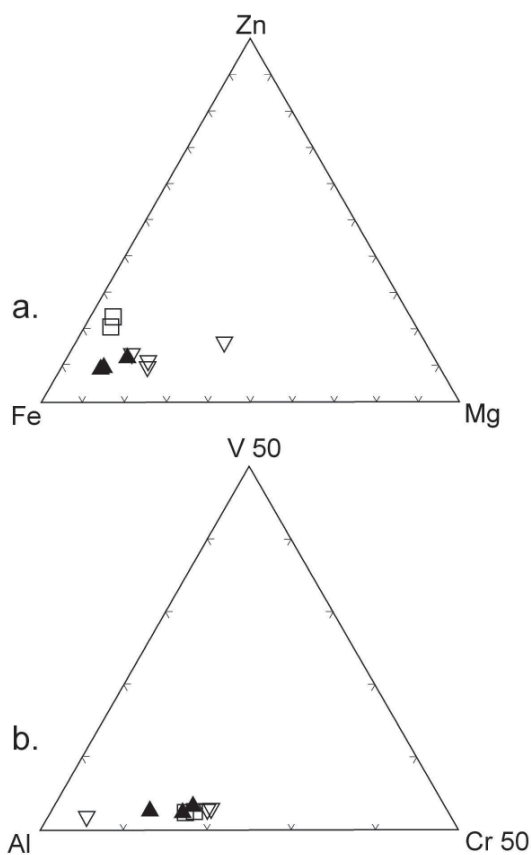


FIG. 5. Plots of hercynite compositions for sample 01–PB–2 (▲). Also shown are compositions of chromian–zincian–vanadoan hercynite from Bernier (1990) (□) and in nearby metapelites, from Keane (1997) (▽). a) Compositional variation in terms of R^{2+} cations; b) variation in terms of R^{3+} cations.

TABLE 3. REPRESENTATIVE COMPOSITIONS OF SILLIMANITE IN METAPELITES FROM THE PARADISE BASIN

	01- PB-1 Incl.	01- PB-2.2 Incl.	01- PB-2.3 Incl.	01- PB-2.4 Incl.	01- PB-2.5 Matrix	01- PB-2.6 Matrix	01- PB-2.7 Matrix
SiO ₂ wt.%	36.74	36.70	36.90	37.01	36.85	37.03	37.00
TiO ₂	0.00	0.00	0.00	0.00	0.01	0.00	0.04
Al ₂ O ₃	62.40	61.91	62.02	61.58	61.85	62.22	62.04
Fe ₂ O ₃	0.83	1.04	1.13	1.12	0.09	0.17	0.13
Mn ₂ O ₃	0.04	0.06	0.05	0.02	0.00	0.00	0.00
V ₂ O ₃	0.33	0.48	0.39	0.56	0.23	0.15	0.12
Cr ₂ O ₃	0.04	0.16	0.03	0.32	0.16	0.16	0.09
Total	100.38	100.35	100.50	100.61	99.19	99.74	99.41
Si <i>apfu</i>	0.995	0.998	1.001	1.007	1.006	1.002	1.004
Ti	0.000	0.000	0.000	0.000	0.000	0.000	0.001
Al	1.992	1.985	1.983	1.975	1.990	1.994	1.992
Fe ³⁺	0.008	0.011	0.011	0.011	0.001	0.002	0.001
Mn	0.000	0.001	0.000	0.000	0.000	0.000	0.000
V	0.004	0.005	0.004	0.006	0.003	0.002	0.001
Cr	0.000	0.002	0.000	0.003	0.002	0.002	0.001

Incl.: sillimanite included in garnet; Matrix: matrix sillimanite grain. Atomic proportions normalized to 2 cations, and expressed as atoms per formula unit (*apfu*).

TABLE 4. REPRESENTATIVE COMPOSITIONS OF GARNET IN METAPELITES FROM THE PARADISE BASIN

	01- PB- 2.1b s.g.c.	01- PB- 2.4b s.g.c.	01- PB- 2.5b s.g.c.	01- PB- 2.2b s.g.r.	01- PB- 2.3b s.g.r.	01- PB- 2.6b s.g.r.	01- PB- 2.7b s.g.r.	01- PB- 2.6a l.g.c.	01- PB- 2.9a l.g.r.
SiO ₂ wt.%	37.69	37.41	37.74	37.75	37.94	37.61	37.63	38.03	37.83
Al ₂ O ₃	21.21	21.39	21.28	21.67	21.43	21.19	21.47	21.27	20.88
TiO ₂	0.00	0.00	0.00	0.00	0.00	0.00	0.00	0.00	0.00
Cr ₂ O ₃	0.19	0.13	0.19	0.23	0.24	0.13	0.18	0.20	0.25
V ₂ O ₃	0.05	0.07	0.06	0.09	0.01	0.07	0.07	0.01	0.01
FeO	34.11	34.49	33.92	34.86	34.06	34.92	34.95	32.96	33.92
MnO	0.89	0.92	1.05	0.90	0.89	0.90	1.13	0.88	0.99
MgO	4.30	4.33	4.27	4.18	4.10	3.91	3.53	5.18	4.27
CaO	1.02	1.03	0.99	1.05	1.13	1.11	1.12	1.01	1.29
ZnO	0.00	0.00	0.00	0.07	0.05	0.02	0.02	0.00	0.00
Total	99.47	99.77	99.50	100.79	99.85	99.86	100.12	99.57	99.50
Si <i>apfu</i>	3.016	2.992	3.017	2.990	3.022	3.010	3.007	3.031	3.039
Al	2.000	2.016	2.006	2.023	2.012	1.999	2.022	1.998	1.977
Ti	0.000	0.000	0.000	0.000	0.000	0.000	0.000	0.000	0.000
Cr	0.012	0.009	0.012	0.014	0.015	0.008	0.012	0.013	0.016
V	0.004	0.004	0.004	0.005	0.000	0.005	0.005	0.000	0.000
Fe	2.283	2.307	2.268	2.310	2.269	2.338	2.335	2.198	2.279
Mn	0.061	0.062	0.071	0.060	0.060	0.061	0.076	0.059	0.068
Mg	0.513	0.517	0.509	0.494	0.487	0.466	0.421	0.615	0.511
Ca	0.087	0.088	0.085	0.089	0.096	0.095	0.096	0.086	0.111
Zn	0.000	0.000	0.000	0.004	0.003	0.001	0.001	0.000	0.000
X _{Alm}	0.78	0.78	0.77	0.78	0.78	0.79	0.80	0.75	0.77
X _{Prp}	0.17	0.17	0.17	0.17	0.17	0.16	0.14	0.20	0.17
X _{Grs}	0.03	0.03	0.03	0.03	0.03	0.03	0.03	0.03	0.04
X _{Sps}	0.02	0.02	0.02	0.02	0.02	0.02	0.02	0.02	0.02
Mg/Fe	0.18	0.18	0.18	0.18	0.18	0.17	0.15	0.22	0.18

Analytical results are normalized to 8 cations. Abbreviations: s.g.c.: small garnet, core; s.g.r.: small garnet, rim; l.g.c.: large garnet, core; l.g.r.: large garnet, rim.

$$K_D \frac{Grt}{Ilm} = \left(\frac{\frac{Mg}{Fe} Grt}{\frac{Mg}{Fe} Opx} \cdot \frac{\frac{Mg}{Fe} Opx}{\frac{Mg}{Fe} Ilm} \right)$$

The K_D value for grt-ilm at 800°C is approximately 5.4. Application of this K_D with the assumption that the Mg/Fe in garnet rims is not reset generates a peak composition for matrix ilmenite of approximately Ilm₃₉Gkl₉Hem₂Kar₁ compared to the Ilm₉₆Gkl₂Hem₂Kar₁ that is now preserved. The more magnesian ilmenite composition was used in GRIPS barometry.

Cordierite

Cordierite is the most abundant matrix phase in sample 01-PB-2. Some grains form a symplectitic intergrowth with plagioclase (Fig. 3), though most appear as large subhedral matrix grains. Optically, the cordierite lacks the characteristic pleochroic halos, and it is difficult to distinguish from plagioclase. The cordi-

TABLE 5. REPRESENTATIVE COMPOSITIONS OF BIOTITE IN METAPELITES FROM THE PARADISE BASIN

	01-PB -2.1 Incl.	01-PB -2.2 Incl.	01-PB -2.6 Matrix	01-PB -2.8 Matrix	01-PB -2.10 Incl. in Qtz
SiO ₂ wt.%	37.74	37.30	35.19	35.13	34.49
Al ₂ O ₃	18.63	18.47	20.46	20.31	17.60
TiO ₂	2.17	2.12	2.24	2.24	5.19
Cr ₂ O ₃	0.50	0.50	0.26	0.20	0.44
V ₂ O ₅	1.03	1.00	0.21	0.23	0.41
Fe ₂ O ₃	0.57	0.54	0.71	0.72	0.80
FeO	12.25	11.71	15.36	15.46	17.35
MnO	0.02	0.01	0.04	0.09	0.04
MgO	13.74	14.06	11.12	11.28	8.23
CaO	0.02	0.01	0.03	0.05	0.00
K ₂ O	7.39	8.24	9.23	9.17	9.17
Na ₂ O	0.27	0.34	0.16	0.16	0.14
Cl	0.26	0.26	0.09	0.09	0.25
F	0.18	0.15	0.00	0.00	0.08
Total	94.77	94.71	95.07	95.13	94.21
Si <i>apfu</i>	5.482	5.443	5.262	5.254	5.285
Al	3.196	3.177	3.606	3.579	3.178
Ti	0.237	0.233	0.252	0.252	0.599
Cr	0.058	0.057	0.031	0.024	0.053
V	0.119	0.116	0.025	0.028	0.051
Fe ³⁺	0.062	0.060	0.080	0.081	0.093
Fe ²⁺	1.488	1.429	1.921	1.934	2.224
Mn	0.002	0.001	0.004	0.011	0.005
Mg	2.976	3.059	2.480	2.516	1.881
Ca	0.003	0.002	0.005	0.008	0.000
K	1.370	1.534	1.760	1.750	1.793
Na	0.077	0.097	0.045	0.046	0.042
Cl	0.065	0.063	0.023	0.024	0.064
F	0.081	0.071	0.000	0.000	0.040
OH	2.375	2.375	2.425	2.425	2.285
Mg#	66.7	68.2	56.3	56.5	45.8

Fe³⁺ estimated as Fe³⁺ = Fe total * 0.04, from Guidotti & Dyer (1991). Atomic proportions calculated on the basis of 22 atoms of oxygen.

erite in this sample is unzoned and is approximately Crd₆₈Skn₃₂ (Table 9).

DISCUSSION

K_D relationships

Distribution coefficients (K_D) for V and Cr were calculated for pairs of coexisting minerals; cation concentrations have been normalized to Al for relative comparison. The general equation used for calculation of the distribution coefficients is:

$$K_D^{(V,Cr)} = \frac{X_{(V,Cr)}^{(Y)}}{X_{(V,Cr)}^{(Z)}} \cdot \frac{X_{(Al)}^{(Z)}}{X_{(Al)}^{(Y)}}$$

where X is the mole fraction of Al, V or Cr in minerals Y and Z. Figure 7a shows V and Cr contents for sillimanite inclusions and host garnet. Vanadium is partitioned nearly equally between sillimanite and garnet ($K_D^{V_{Grt/Sil}} = 0.98$), and Cr is strongly partitioned into garnet ($K_D^{Cr_{Grt/Sil}} = 6.9$). As expected, V and Cr are very strongly partitioned into hercynite over both sillimanite and garnet (Figs. 7b, c). The V and Cr are likely depleted in the matrix of the rock by Rayleigh fractionation during early crystallization of garnet, hercynite and

TABLE 6. REPRESENTATIVE COMPOSITIONS OF THE FELDSPARS IN METAPELITES FROM THE PARADISE BASIN

	01-PB-2.5 Matrix	01-PB-2.6 Matrix	01-PB-2.3 Incl./sm grt	01-PB-2.2 Matrix
SiO ₂ wt.%	63.47	64.08	60.02	59.37
Al ₂ O ₃	18.71	18.89	24.32	25.13
Fe ₂ O ₃	0.05	0.00	0.47	0.10
K ₂ O	15.62	14.75	0.11	0.13
Na ₂ O	0.71	1.46	8.56	8.03
CaO	0.00	0.02	5.72	6.52
MnO	0.00	0.00	0.00	0.00
MgO	0.00	0.00	0.02	0.00
BaO	0.47	0.39	0.00	0.00
SrO	0.00	0.00	0.00	0.00
Total	99.04	99.58	99.22	99.27
Si <i>apfu</i>	2.971	2.971	2.680	2.655
Al	1.032	1.030	1.280	1.324
Fe ³⁺	0.002	0.000	0.016	0.003
K	0.933	0.870	0.009	0.010
Na	0.065	0.131	0.741	0.696
Ca	0.000	0.001	0.274	0.312
Mn	0.000	0.000	0.000	0.000
Mg	0.001	0.000	0.001	0.000
Ba	0.009	0.007	0.000	0.000
Sr	0.000	0.000	0.000	0.000
X Kfs	0.93	0.87	0.01	0.01
X Ab	0.06	0.13	0.72	0.70
X An	0.00	0.00	0.27	0.31

Cations normalized to 5 atoms. Incl./sm grt: inclusion in small grain of garnet.

TABLE 7. REPRESENTATIVE COMPOSITIONS OF SPINEL IN METAPELITES FROM THE PARADISE BASIN

	01-PB-2.3 Matrix	01-PB-2.4 Matrix	01-PB-2.5 Inclusion
Al ₂ O ₃ wt. %	44.83	44.88	47.86
Cr ₂ O ₃	12.58	13.02	9.97
V ₂ O ₅	2.47	2.61	2.39
FeO	32.46	32.64	29.82
Fe ₂ O ₃	0.81	0.57	0.57
MgO	2.35	2.26	3.38
ZnO	4.44	4.29	5.67
TiO ₂	0.00	0.00	0.00
SiO ₂	0.00	0.00	0.02
MnO	0.00	0.00	0.00
Total	99.95	100.28	99.68
Al <i>apfu</i>	1.586	1.587	1.671
Cr	0.299	0.309	0.235
V	0.060	0.063	0.057
Fe ²⁺	0.815	0.819	0.739
Fe ³⁺	0.037	0.026	0.026
Mg	0.105	0.101	0.149
Zn	0.099	0.095	0.124
Ti	0.000	0.000	0.000
Si	0.000	0.000	0.000
Mn	0.000	0.000	0.000
Usp	0.0	0.0	0.0
Spl	10.5	10.1	14.9
Gal	0.0	0.0	0.0
Chr	14.9	15.5	11.7
Ghn	9.9	9.5	12.4
Hc	59.4	59.9	56.3
Mgt	1.8	1.3	1.3
Cou	3.0	3.1	2.8
Mg #	0.1	0.1	0.2

Cations normalized to 3 atoms. Symbols: Chr: chromite, Cou: coulsonite, (Fe³⁺V₂O₅), Gal: galaxite, Ghn: gahnite, Hc: hercynite, Mgt: magnetite, Spl: spinel, Usp: ulvöspinel.

TABLE 8. REPRESENTATIVE COMPOSITIONS OF ILMENITE AND RUTILE IN METAPELITES FROM THE PARADISE BASIN

	01-PB-2.1 Ilmenite Matrix	01-PB-2.2 Ilmenite Inclusion	01-PB-2.1a Rutile Matrix
Al ₂ O ₃ wt. %	0.01	0.00	0.01
Cr ₂ O ₃	0.07	0.12	0.17
V ₂ O ₅	0.75	0.75	1.28
FeO	43.60	45.41	-
Fe ₂ O ₃	1.73	0.92	0.84
MgO	0.10	0.61	0.00
ZnO	0.00	0.60	-
TiO ₂	50.81	50.43	97.02
SiO ₂	0.02	0.00	0.10
MnO	1.21	0.17	0.01
Nb ₂ O ₅	0.11	0.17	-
H ₂ O	-	-	0.31
Total	98.42	98.58	99.73
Al <i>apfu</i>	0.000	0.000	0.000
Cr	0.002	0.002	0.002
V	0.016	0.016	0.016
Fe ²⁺	0.939	0.975	-
Fe ³⁺	0.067	0.035	0.010
Mg	0.004	0.023	-
Zn	0.000	0.000	-
Ti	0.984	0.974	0.971
Si	0.019	0.000	0.001
Mn	0.026	0.004	0.000
Nb	0.001	0.001	-
H	-	-	0.028
Mg #	0.004	0.023	0.000

H calculated from charge balance. Ilmenite compositions are normalized to 2 cations, whereas the composition of rutile is normalized to 1 cation. The included grain of ilmenite is enclosed in garnet.

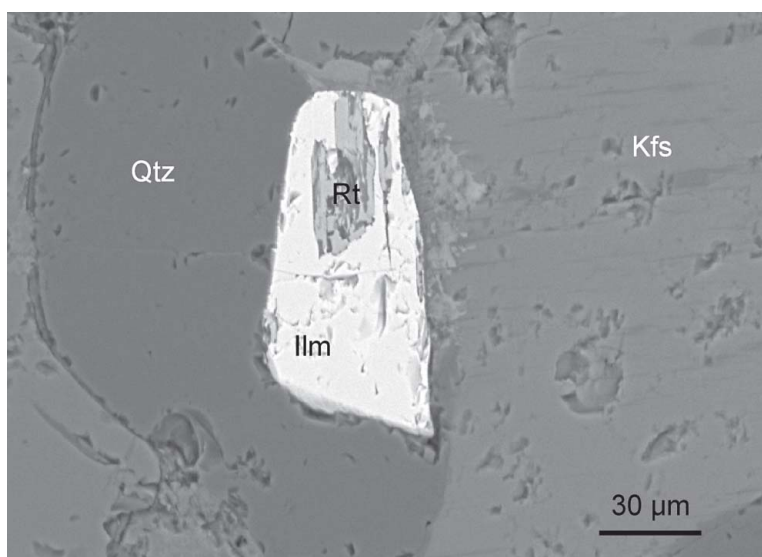


FIG. 6. BSE image of rutile included in and rimmed by ilmenite from the matrix of 01-PB-2.

sillimanite, similar to the commonly observed depletion of Mn in growing garnet (Hollister 1966).

Minor element substitutions in sillimanite may perturb thermobarometric calculations involving the aluminosilicate polymorphs (Strens 1968, Kerrick & Speer 1988). Minor dilution by transition-metal elements produces relatively large displacements in the positions of Al_2SiO_5 equilibria in P–T space. For example, if the activity of Al_2SiO_5 in sillimanite is reduced to 0.98 (the value obtained using an ideal model for the observed substitution of V, Cr and Fe in the sillimanite inclusions), the reaction $\text{And} = \text{Sil}$ is calculated to shift by -0.7 kbar at 500°C compared to the pure Al_2SiO_5 system. However, the available data (Strens 1968, Okrusch & Evans 1970) suggest that V preferentially substitutes into andalusite and Cr enters kyanite, which means that the effect of V and Cr on sillimanite stability is offset by concomitant substitutions in the other polymorphs. Andalusite usually prefers Fe over sillimanite (Strens 1968, Okrusch & Evans 1970, Pattison 1992, Sepahi *et al.* 2004), although Kerrick (1987) observed that Fe favors andalusite over “fibrolite”. The effect of the observed reduced activity of Al_2SiO_5 in sillimanite on calculated pressure for other thermobarometers is minor. For example, at 700°C , the GASP boundary is shifted by -0.1 kbar, and the GRAIL boundary, by $+0.1$ kbar.

Kerrick & Speer (1988) argued for a positive correlation between redox state and incorporation of Fe, Mn, Cr, V, and Ti in the aluminosilicates, such that under highly oxidized conditions, the aluminosilicates become more enriched in these elements. However, oxidation of Cr and V would produce soluble species that are more

easily mobilized in an aqueous fluid before or during a metamorphic event, which indeed could provide a mechanism of transport for these elements if they were introduced metasomatically. Sillimanite from sample 01–PB–2 is in equilibrium with graphite and is therefore relatively reduced, yet contains high levels of V, Cr, and Fe. Thus, oxidation state alone for a given rock is a poor predictor of minor element content in the aluminosilicates.

The origin of the V and Cr in the metapelites of the WRR is not entirely evident. There is no evidence of the introduction of elements along veins or fractures either in the field or in thin section. Secco *et al.* (2002) reported Cr- and V-rich sodic clinopyroxenes rimming eskolaite (Cr_2O_3) and karelianite (V_2O_5) from granulites of the Sludyanka Complex, Siberia. Although no similar detrital V–Cr oxides have been identified in the metapelites of the WRR, it is possible that they existed in the rocks prior to recrystallization. However, it seems more probable to us that the Cr is derived from clastic chromite and the V from decomposition of micas or clay minerals. Such minerals likely were derived from weathering of Archean metagranitic rocks and minor mafic and ultramafic units, some of which occur directly adjacent to the metapelites. It is also possible that V and Cr became concentrated in aluminous clays during premetamorphic hydrothermal alteration (Bernier 1990), although there is no corroborating evidence for this process in the field. The enrichment of Cr, V and Zn together could be produced by metasomatic alteration of komatiitic rocks (G.N. Phillips, pers. commun., 2003). Canet *et al.* (2003) described even greater enrichments of V and Cr in contact-metamorphosed black shales from Catalonia, Spain, and identified the source of these metals as being the black shale. Black shales could represent the protolith of the Paradise Basin metapelites.

P–T conditions and tectonic implications

Three separate sets of P–T conditions, delineated by textural evidence, have been calculated for sample 01–PB–2. The internally consistent database of Holland & Powell (1998) was used to determine the P–T positions of reactions used. The quaternary-solid-solution mixing model of Ganguly *et al.* (1996) was used to determine the activity – composition relations for garnet.

Inclusion assemblage

The presence of rutile in the core of ilmenite from the matrix of sample 01–PB–2 indicates early high-pressure conditions. The GRAIL barometer ($\text{Alm} + 3 \text{Rt} = \text{Sil} + 3 \text{Ilm} + 2 \text{Qtz}$) was calculated assuming ideal ilmenite (as this phase is absent in the sample) and using the compositions of the rutile and the core of the large garnet porphyroblasts. This reaction yields a lower pressure limit of 9.5 kbar at 800°C (Fig. 8a). The tempera-

TABLE 9. REPRESENTATIVE COMPOSITIONS OF CORDIERITE IN METAPELITES FROM THE PARADISE BASIN

	01-Pb -2.1	01-Pb -2.2	01-Pb -2.3	01-Pb -2.4	01-Pb -2.5	01-Pb -2.6
SiO_2 wt. %	48.52	49.34	48.54	48.51	48.41	47.99
Al_2O_3	33.38	32.98	33.21	33.14	32.86	33.15
Fe_2O_3	0.14	0.11	0.15	0.29	0.07	0.04
FeO	7.21	7.14	7.34	7.43	7.33	7.59
MnO	0.07	0.05	0.05	0.05	0.04	0.04
MgO	9.10	9.17	8.99	8.95	8.91	8.73
CaO	0.02	0.01	0.01	0.01	0.08	0.02
Na_2O	0.06	0.06	0.06	0.07	0.11	0.08
K_2O	0.00	0.00	0.00	0.01	0.01	0.00
Total	98.49	98.86	98.37	98.44	97.82	97.62
Si	4.958	5.025	4.971	4.968	4.989	4.957
Al	4.020	3.959	4.009	4.000	3.992	4.035
Fe^{3+}	0.010	0.010	0.010	0.030	0.010	0.000
Fe^{2+}	0.610	0.610	0.630	0.630	0.630	0.660
Mn	0.006	0.005	0.005	0.004	0.004	0.003
Mg	1.386	1.393	1.373	1.366	1.369	1.345
Ca	0.002	0.001	0.001	0.001	0.009	0.002
Na	0.005	0.006	0.006	0.007	0.011	0.008
K	0.000	0.000	0.000	0.001	0.001	0.000

Cations normalized to 7 atoms.

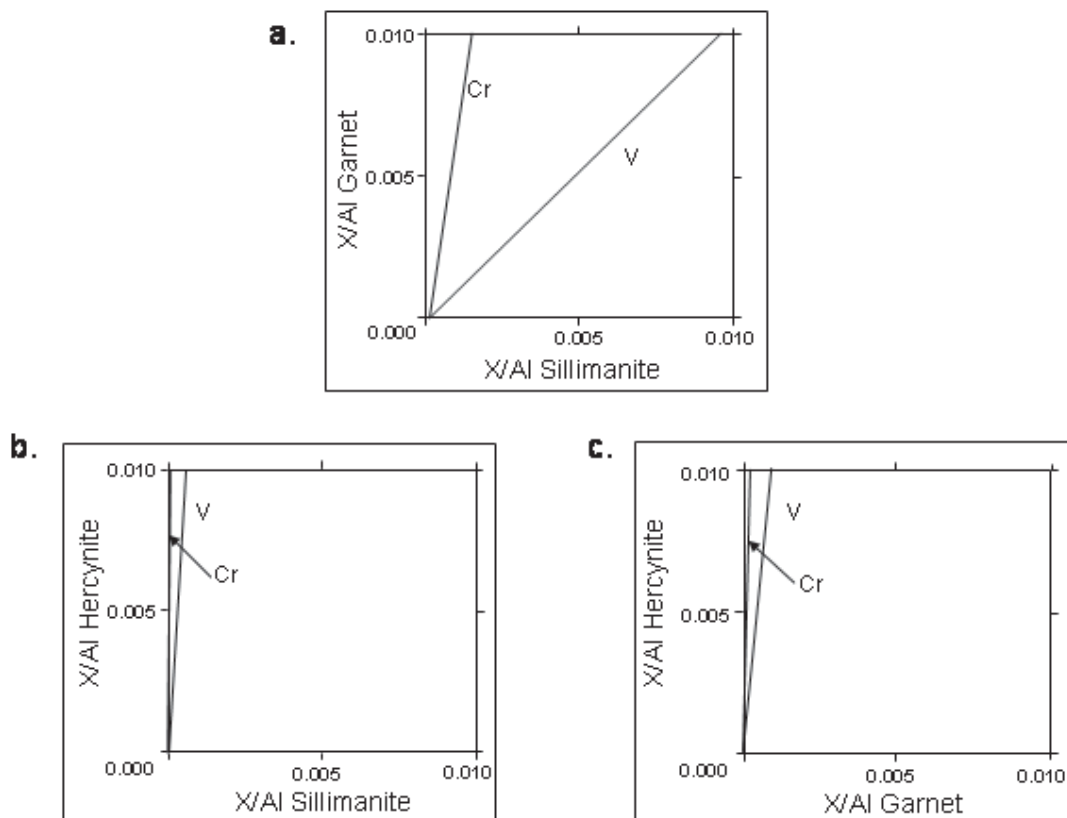
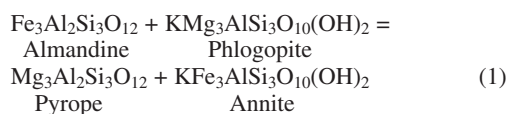


FIG. 7. Distribution of V and Cr among the coexisting phases garnet, sillimanite and hercynite. Cr and V contents of each phase are shown as a ratio of X/Al , where X represents the mole fraction of Cr or V.

ture for this portion of the P–T history was not directly determined.

Core of matrix minerals

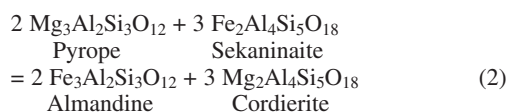
Coexisting garnet and biotite from the matrix were utilized to recover temperature in the sample *via* the reaction:



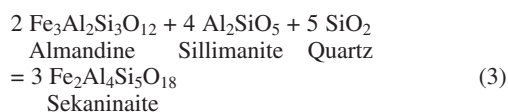
Compositions of garnet cores from the small porphyroblasts paired with biotite inclusions in quartz from the matrix yield temperatures above 750°C. Pressure is limited to <9.5 kbar *via* the GRAIL reaction in the absence of rutile (Fig. 8b). The elevated levels of Ti in biotite grains included in quartz (up to 5.19 wt%) also suggests a high-temperature history.

Rim of matrix minerals

Temperatures have been determined for the rim compositions of the matrix assemblages *via* both garnet–biotite and garnet–cordierite Mg–Fe exchange reactions. Using the reaction:



temperatures have been estimated at ~650°C (Fig. 8c). The stability of cordierite in the presence of garnet, sillimanite, and quartz yields pressures of <5 kbar *via* the reaction:



Garnet–biotite temperature estimates for rim compositions in the matrix yield even lower temperatures, ~500°C. The biotite and garnet continued to exchange Mg and Fe after cordierite was closed to diffusion.

The calculated P–T conditions for the granulites of Paradise Basin place them among the highest-pressure metamorphic rocks in the WRR. Frost *et al.* (2000) reported peak temperatures of 750°C and lower pressure limits of 6 kbar from granulites at Burnt Lake, 25 km west of the Paradise Basin. Sharp & Essene (1991) documented inclusion assemblages in the northernmost WRR with conditions of 815°C and 8 kbar and matrix assemblages at 650–750°C and 5.5 kbar. Their data are similar to those found here in recording much higher P–T conditions using mineral inclusions in garnet than in matrix assemblages.

The combination of these three distinct P–T conditions allows for estimation of the retrograde P–T path. Figure 9 shows part of a possible clockwise P–T path

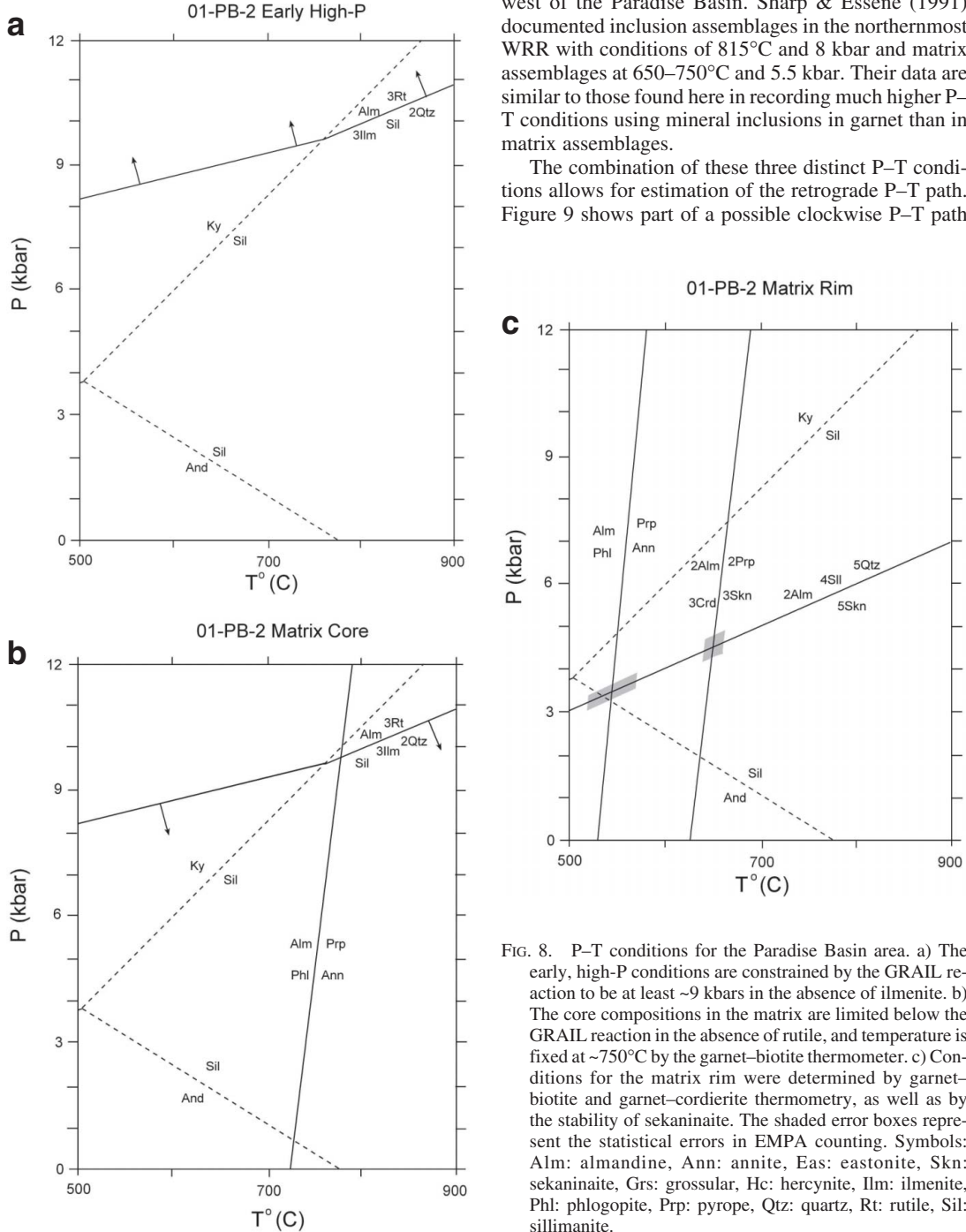


FIG. 8. P–T conditions for the Paradise Basin area. a) The early, high-P conditions are constrained by the GRAIL reaction to be at least ~9 kbars in the absence of ilmenite. b) The core compositions in the matrix are limited below the GRAIL reaction in the absence of rutile, and temperature is fixed at ~750°C by the garnet–biotite thermometer. c) Conditions for the matrix rim were determined by garnet–biotite and garnet–cordierite thermometry, as well as by the stability of sekaninaite. The shaded error boxes represent the statistical errors in EMPA counting. Symbols: Alm: almandine, Ann: annite, Eas: eastonite, Skn: sekaninaite, Grs: grossular, Hc: hercynite, Ilm: ilmenite, Phl: phlogopite, Prp: pyrope, Qtz: quartz, Rt: rutile, Sil: sillimanite.

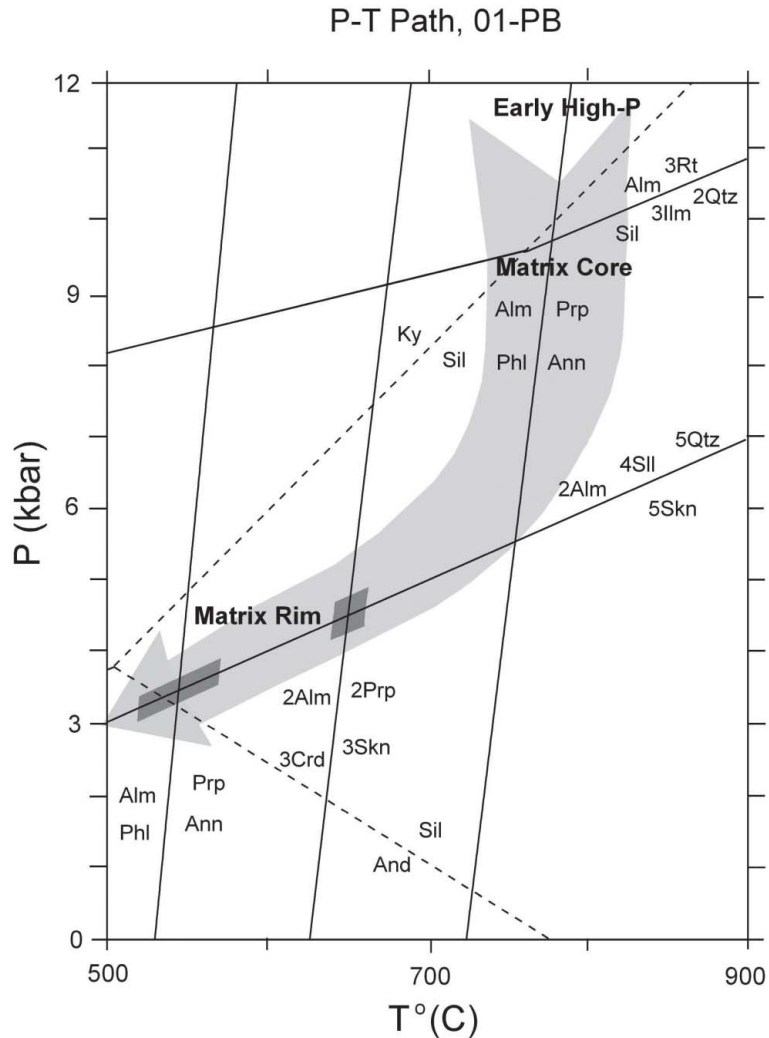


FIG. 9. Possible P-T path for rocks from the Paradise Basin.

for the rocks of the Paradise Basin, which is similar to the path constructed by Sharp & Essene (1991) for the northernmost WRR using inclusion and matrix assemblages. They interpreted their P-T path to represent the slow cooling of a single, long-lived metamorphic event. Whereas this interpretation also seems plausible for our data, the possibility of multiple metamorphic events cannot be discounted. In other words, two or more clockwise P-T curves could be constructed to fit the data in Figure 9. Frost *et al.* (2000) argued for at least four late Archean metamorphic events, primarily on the basis of preserved fabrics related to deformational events and ages of adjacent plutons, although the relationship

between the plutons and adjacent metamorphic rocks is not always clear. Additional chronological data on the metamorphic units are needed to better constrain the hypothesis that multiple metamorphic events and P-T paths are warranted.

If the P-T history is assumed to have been a single event, tectonic scenarios for the formation of the granulites can be constructed from the nature of the retrograde path. The path for the Paradise Basin is similar in character to those described by Harley (1989) as exhibiting "isothermal decompression", which implies a history of tectonic thickening of the crust followed by rapid tectonic denudation or erosion (Bohlen 1987). Thus, the Archean metamorphism of the WRR, or at least the

Paradise Basin area, was not controlled by the emplacement of the igneous rocks.

As an alternative, multiple pulses of metamorphism could be employed to explain the pattern of preserved P–T conditions. In this scenario, one might expect that the high-grade conditions preserved in garnet cores represent an early event due to deep burial, whereas the lower-grade conditions represent a second lower-pressure thermal event. The lower-pressure event may be related to heating related to the intrusion of the adjacent Louis Lake Batholith or by thinning of the crust due to extension.

ACKNOWLEDGEMENTS

This paper is dedicated to Dugald Carmichael for his epochal works on aluminosilicates in metamorphic rocks. He taught us to interpret chemical reactions by looking carefully at textures, and to consider the separate implications of barometry vs. thermometry in metamorphic terranes. We all hope that he will continue to attend national and international meetings so that we can hear his wit and insightful commentary and watch him dance on tables at parties. We thank M.K. Davis for assistance with the Raman apparatus, C. Henderson for assistance with and maintenance of the electron microprobes, and R.C. Rouse for assistance in the X-ray laboratory. We also thank C. Manning, T. Rivers, T. Chacko, N. Bégin and R.F. Martin for reviews of this manuscript. This work was supported by NSF grant EAR 97–06349 to EJE and by a Scott L. Turner Grant from the University of Michigan to CLD. The electron microprobes were purchased by UM from NSF funds with grants EAR 82–12764 and 99–11352 to EJE and the SEM with grant EAR 96–28196 to D.R. Peacor and EJE.

REFERENCES

- BERNIER, L.R. (1990): Vanadiferous zirconian–chromian hercynite in a metamorphosed basalt-hosted alteration zone, Atik Lake, Manitoba. *Can. Mineral.* **28**, 37–50.
- BOHLEN, S.R. (1987): Pressure–temperature–time paths and a tectonic model for the evolution of granulites. *J. Geol.* **95**, 617–632.
- CANET, C., ALFONSO, P., MELGAREJO, J.-C. & JORGE, S. (2003): V-rich minerals in contact-metamorphosed Silurian sedex deposits in the Poblet area, southwestern Catalonia, Spain. *Can. Mineral.* **41**, 561–579.
- COOPER, A.F. (1980): Retrograde alteration of chromian kyanite in metachert and amphibolite whiteschist from the Southern Alps, New Zealand, with implications for uplift on the alpine fault. *Contrib. Mineral. Petrol.* **75**, 153–164.
- DEER, W.A., HOWIE, R.A. & ZUSSMAN, J. (1982): *Rock-Forming Minerals*. **1A. Orthosilicates**. John Wiley & Sons, New York, N.Y.
- DODGE, F.C.W. (1971): Al₂SiO₅ minerals in rocks of the Sierra Nevada and the Inyo Mountains, California. *Am. Mineral.* **56**, 1443–1451.
- FROST, B.R., CHAMBERLAIN, K.R., SWAPP, S., FROST, C.D. & HULSEBOSCH, T.P. (2000): Late Archean structural and metamorphic history of the Wind River Range: evidence for a long-lived active margin on the Archean Wyoming craton. *Geol. Soc. Am., Bull.* **112**, 564–578.
- FROST, C.D., FROST, B.R., CHAMBERLAIN, K.R. & HULSEBOSCH, T.P. (1998): The Late Archean history of the Wyoming Province as recorded by granitic magmatism in the Wind River Range, Wyoming. *Precamb. Res.* **89**, 145–173.
- GANGULY, J., CHENG, W. & TIRONE, M. (1996): Thermodynamics of aluminosilicate garnet solid solution: new experimental data, an optimized model, and thermometric applications. *Contrib. Mineral. Petrol.* **126**, 137–151.
- GIL IBARGUCHI, J.I., MENDIA, M. & GIRARDEAU, J. (1991): Mg- and Cr-rich staurolite and Cr-rich kyanite in high-pressure ultrabasic rocks (Cabo Ortegal, northwestern Spain). *Am. Mineral.* **76**, 501–511.
- GREW, E.S. (1980): Sillimanite and ilmenite from high-grade metamorphic rocks of Antarctica and other areas. *J. Petrol.* **21**, 39–68.
- GUIDOTTI, C.V. & DYAR, M.D. (1991): Ferric iron in metamorphic biotite and its petrologic and crystallochemical implications. *Am. Mineral.* **76**, 161–175.
- HARLEY, S.L. (1989): The origins of granulites: a metamorphic perspective. *Geol. Mag.* **126**, 215–247.
- HAYOB, J.L., BOHLEN, S.R. & ESSENE, E.J. (1993): Experimental investigation and application of the equilibrium rutile + orthopyroxene = quartz + ilmenite. *Contrib. Mineral. Petrol.* **115**, 18–35.
- HOLLAND, T.J.B. & POWELL, R. (1998): An internally consistent thermodynamic dataset for phases of petrological interest. *J. Metamorph. Geol.* **16**, 309–343.
- HOLLISTER, L.S. (1966): Garnet zoning; an interpretation based on the Rayleigh fractionation model. *Science* **154**, 1647–1651.
- KEANE, S.D. (1997): *Preservation of Early Histories in Granulites from Trace Element Zoning in Garnet*. M.Sc. thesis, Univ. of Michigan, Ann Arbor, Michigan.
- KERRICK, D.M. (1987): Fibrolite in contact aureoles of Donegal, Ireland. *Am. Mineral.* **72**, 240–254.
- _____ & SPEER, J.A. (1988): The role of minor element solid solution on the andalusite–sillimanite equilibrium in metapelites and peraluminous granitoids. *Am. J. Sci.* **288**, 152–192.
- LEE, H.K. & GANGULY, J. (1988): Equilibrium compositions of coexisting garnet and orthopyroxene: experimental

- determinations in the system FeO–MgO–Al₂O₃–SiO₂, and applications. *J. Petrol.* **29**, 93-113.
- MORAND, V.J. (1988): Vanadium-bearing margarite from the Lachan Fold Belt, New South Wales, Australia. *Mineral. Mag.* **52**, 341-345.
- OHMOTO, H. & KERRICK, D.M. (1977): Devolatilization equilibria in graphitic systems. *Am. J. Sci.* **277**, 1013-1044.
- OKRUSCH, M. & EVANS, B.W. (1970): Minor element relationships in coexisting andalusite and sillimanite. *Lithos* **3**, 261-268.
- PATTISON, D.R.M. (1992): Stability of andalusite and sillimanite and the Al₂SiO₅ triple point: constraints from the Ballachulish aureole, Scotland. *J. Geol.* **100**, 423-446.
- PERRY, K., JR. (1965): *High Grade Regional Metamorphism of Precambrian Gneisses and Associated Rocks*. Ph.D. thesis, Yale University, New Haven, Connecticut.
- RUDNICK, R.L., BARTH, M., HORN, I. & McDONOUGH, W.F. (2000): Rutile-bearing refractory eclogites: missing link between continents and depleted mantle. *Science* **287**, 278-281.
- SCHULING, R.D. & FEENSTRA, A. (1980): Geochemical behavior of vanadium in iron–titanium oxides. *Chem. Geol.* **30**, 143-150.
- SECCO, L., MARTIGNAGO, F., DAL NEGRO, A., REZNITSKII, L.Z. & SKLYAROV, E.V. (2002): Crystal chemistry of Cr³⁺–V³⁺-rich clinopyroxenes. *Am. Mineral.* **87**, 709-714.
- SEPAHI, A.A., WHITNEY, D.L. & BAHARIFAR, A.A. (2004): Petrogenesis of andalusite – kyanite – sillimanite veins and host rocks, Sanandaj–Sirjan metamorphic belt, Hamadan, Iran. *J. Metamorph. Geol.* **22**, 119-134.
- SHARP, Z.D. & ESSENE, E.J. (1991): Metamorphic conditions of an Archean core complex in the northern Wind River Range, Wyoming. *J. Petrol.* **32**, 241-273.
- SOBOLEV, N.B., JR., KUZENETSOVA, I.K. & ZYUZIN, N.I. (1968): The petrology of groszpydite xenoliths from the Zagadochnaya kimberlite pipe in Yakutia. *J. Petrol.* **9**, 253-280.
- STRENS, R.G.J. (1968): Stability of Al₂SiO₅ solid solutions. *Mineral. Mag.* **36**, 839-849.
- VRANA, S., RIEDER, M. & PODLAHA, J. (1978): Kanonaite (Mn³⁺_{0.76}Al_{0.23}Fe³⁺_{0.02})^[6]Al^[5][O/SiO₄], a new mineral isotypic with andalusite. *Contrib. Mineral. Petrol.* **66**, 325-332.
- WANG, L., ESSENE, E.J. & ZHANG, Y. (1999): Mineral inclusions in pyrope crystals from Garnet Ridge, Arizona, USA: implications for processes in the upper mantle. *Contrib. Mineral. Petrol.* **135**, 164-178.


Received September 10, 2003, revised manuscript accepted June 22, 2004.

APPENDIX A. ELECTRON-MICROPROBE METHODS

All phases were studied by back-scattered electron (BSE) imaging and analyzed with a Cameca CAMEBAX electron microprobe using a wavelength-dispersion system and the crystals OV60, PET, TAP and LIF. A PAP correction routine provided by Cameca was used to reduce all sets of analytical data. Samples were analyzed utilizing a focused point-beam with an accelerating voltage of 15 kV and a beam current of 10 nA. The standards used are well-characterized natural and synthetic materials at the University of Michigan. The standards used to analyze garnet are: almandine (Fe, Al, Si), geikielite (Mg, Ti), rhodonite (Mn), uvarovite (Cr), V_2O_5 (V), wollastonite (Ca), YAG (Y), sphalerite (Zn) and zircon (Zr). The standards used to analyze ilmenite, hercynite and sillimanite are: albite (Na), almandine (Fe), andalusite (Al, Si), forsterite (Mg), geikielite (Ti), rhodonite (Mn), uvarovite (Cr), V_2O_5 (V), and sphalerite (Zn). The standards used to analyze biotite are: almandine (Fe, Al), apatite (Cl), geikielite (Mg, Ti), hornblende (K, Na), pyroxene (Si, Ca), topaz (F), uvarovite (Cr), and V_2O_5 (V).

The wavelength interference between $TiK\alpha$ and $VK\alpha$ was minimized by analyzing the samples for V on the LiF crystal, which gives much narrower peak-widths than the PET crystal. The interference was assessed by analyzing synthetic geikielite ($MgTiO_3$) and rutile (TiO_2) standards as unknowns for V, where the amount of fictive vanadium contributed by $TiK\beta$ is $V \text{ wt}\% = 0.0023 * Ti \text{ wt}\%$. Wavelength-peak interferences between $VK\beta$ and $CrK\alpha$ were addressed by analyzing V_2O_5 (a Cr-free synthetic standard) as an unknown for Cr. The ratio of the known wt% V and the apparent wt% Cr in the analysis was then used as a correction factor and applied to the analytical data. This technique yielded a 2.0% correction for synthetic V_2O_5 using a LiF crystal (fictive Cr wt% = $0.020 * V \text{ wt}\%$). The same method of correction was also applied to interferences between $CrK\beta$ and $MnK\alpha$, where a uvarovite standard was analyzed as an unknown for Cr and Mn with a LiF crystal. This procedure yielded a correction of less than 0.01%, and therefore is negligible.

An International Magazine
to keep abreast of the latest developments in mineralogy, geochemistry, and petrology



Elements

An International Magazine of Mineralogy, Geochemistry, and Petrology

March 2005
Volume 1, Number 2
ISSN 1811-5209

Diamonds

- Inclusions in Diamonds – Glimpses into Deep Earth
- Stable Isotopes and the Origin of Diamonds
- Strange Diamonds: Carbonado and Framesite
- Microdiamonds in Metamorphic Rocks
- Meteoritic Nanodiamonds
- Treatment of Gem Diamonds
- Growing Diamonds



Elements

An International Magazine of Mineralogy, Geochemistry, and Petrology

January 2005
Volume 1, Number 1
ISSN 1811-5209

Fluids in Planetary Systems

- Ore-Forming Fluids
- Volatiles in Magmatic-Volcanic Systems
- Water in the Mantle
- Fluids, Faulting, and Flow
- Extraterrestrial Water

To receive *Elements*, join anyone of the participating societies:

- Mineralogical Society of America,
- Mineralogical Society of Great Britain and Ireland,
- The Clay Minerals Society,
- Mineralogical Association of Canada,
- Geochemical Society,
- European Association for Geochemistry,
- International Association of GeoChemistry

www.elementsmagazine.org

THEMES TO COME
IN 2005

- Origin of Life
- Toxic Metals
- Large Igneous Provinces

We acknowledge the financial support of the Government of Canada, through the Publications Assistance Program (PAP), toward our mailing costs.

PUBLICATIONS MAIL AGREEMENT NO. 40011842 • REGISTRATION NO. 09397
RETURN UNDELIVERABLES CANADIAN ADDRESSES TO CIRCULATION DEPT.
330-123 MAIN STREET, TORONTO ON M5W 1A1

Email: circdept@publisher.com